REVIEWS

Journal of Semiconductors
(2023) 44, 031701
doi: 10.1088/1674-4926/44/3/031701

The recent progress of laser-induced graphene based device applications

Liqiang Zhang‡, Ziqian Zhou‡, Xiaosong Hu†, and Liaoyong Wen†

Key Laboratory of 3D Micro/Nano Fabrication and Characterization of Zhejiang Province, School of Engineering, Westlake University, Hangzhou 310024, China

Abstract: Laser writing is a fast and efficient technology that can produce graphene with a high surface area, whereas laser-induced graphene (LIG) has been widely used in both physics and chemical device application. It is necessary to update this important progress because it may provide a clue to consider the current challenges and possible future directions. In this review, the basic principles of LIG fabrication are first briefly described for a detailed understanding of the lasing process. Subsequently, we summarize the physical device applications of LIGs and describe their advantages, including flexible electronics and energy harvesting. Then, chemical device applications are categorized into chemical sensors, supercapacitors, batteries, and electrocatalysis, and a detailed interpretation is provided. Finally, we present our vision of future developments and challenges in this exciting research field.

Key words: laser-induced graphene; flexible electronics; energy harvesting; chemical sensors; supercapacitors; electrocatalysis

Citation: L Q Zhang, Z Q Zhou, X S Hu, and L Y Wen, The recent progress of laser-induced graphene based device applications[J]. *J. Semicond.*, 2023, 44(3), 031701. https://doi.org/10.1088/1674-4926/44/3/031701

1. Introduction

Graphene is an important material with high electronic mobility, flexibility, specific area, mechanical strength, and biocompatibility[1–3]. As a multifunctional material, graphene and its derivatives are very promising in many fields especially in biosensor[4–7], mainly due to the 6-membered carbon ring array structure of graphene. This structure allows it to be connected to a molecule with a benzene ring through a π–π bond, which is feasible to further connect amino-rich aptamers or antibodies as efficient biosensors[6, 7]. So far, the common synthetic methods of graphene include mechanical exfoliation[8], chemical reduction[9] and chemical vapor deposition (CVD)[10, 11]. However, mechanical exfoliation can produce only small pieces of graphene[8], while large area graphene can be fabricated by CVD on desired Cu or Ni substrates with a significantly improved efficiency. However, specific substrates and high-temperature processes are needed for the CVD process[10], which limits its massive application.

In 2014, a new graphene synthesis method named laser-induced graphene (LIG) was discovered by Tour[12]. To put it simply, a high-power CO_2 laser is used to engrave polyimide (PI), the surface part of the PI is then carbonized, of which graphene accounts for a large proportion. The synthesized LIG exhibits high surface area (≈340 m^2/g), high thermal stability (>900 °C), and excellent conductivity (5–25 S/cm)[12]. Because of the cheap raw materials and fast preparation speed, LIG is very suitable for mass production. Other substrates such as wood[13], phenolic resin[14] , and clothes[5] have since been discovered to have similar properties, although PI was the most widely used substrate. The LIG could lower the threshold of graphene applications for many fields due to its abundantly multiscale-level porous structures, which results in a higher charge storage capacity[15] and electrochemical activity in a liquid phase[16]. Therefore, LIG, as an important type of graphene, has demonstrated a potential for practical applications.

In the past few years, several reviews have aimed to give a comprehensive summary and outlook regarding the fabrication and application of LIG and its composites, including physical sensors[17, 18] and energy storage[19] fields. Due to the easy fabrication process and multi-faceted performance, LIG-based devices have exhibited an obvious superiority over other graphene-based devices in many fields and their applications are still expanding. However, a summary related to this aspect is still lacking. A lot of distinctive and interesting research based on LIG devices has recently been published, such as nanogenerators[20] and electrochemical biosensors[21]. Therefore, it is very necessary to update this important progress because it may provide a clue to consider the current challenges and the possible future directions. Consequently, in this review, the formation mechanism of LIG is introduced first to give readers a deeper understanding of the lasing process, so that the LIG can be easily adjusted to different types by controlling laser parameters and atmosphere according to requirement, which is suitable for multifunctional applications. Then, the latest developments of the physical and chemical devices based on LIG technique are summarized in detail, as shown in Fig. 1. Considering that the applications of LIG are so diverse, biochemical sensors, energy storage devices, and electrocatalysts are classified into chemical devices, while flexible electronics (e.g., stretch sensor and temperature sensor) and energy harvesting constitutes are categorized as physical devices. Finally, a summary and perspective view re-

Liqiang Zhang and Ziqian Zhou contributed equally to the work.

Correspondence to: X S Hu, huxiaosong@westlake.edu.cn; L Y Wen, wenliaoyong@westlake.edu.cn

Received 2 SEPTEMBER 2022; Revised 19 SEPTEMBER 2022.

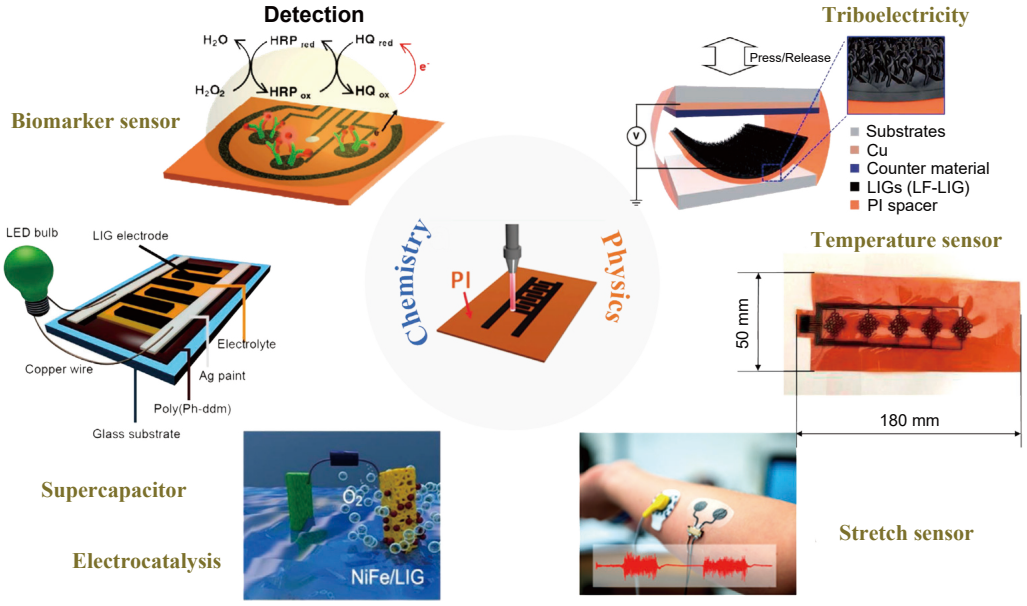

Fig. 1. (Color online) Representative chemical applications of LIG. Adapted with permission from Ref. [22–24]. Copyright 2016, Wiley-VCH, Copyright 2022, American Chemical Society, Copyright 2020, Elsevier Ltd respectively. Representative physical applications of LIG. Adapted with permission from Ref. [25–27]. Copyright 2020, The Royal Society of Chemistry. Copyright 2021, Hindawi. Copyright 2020, American Chemical Society respectively.

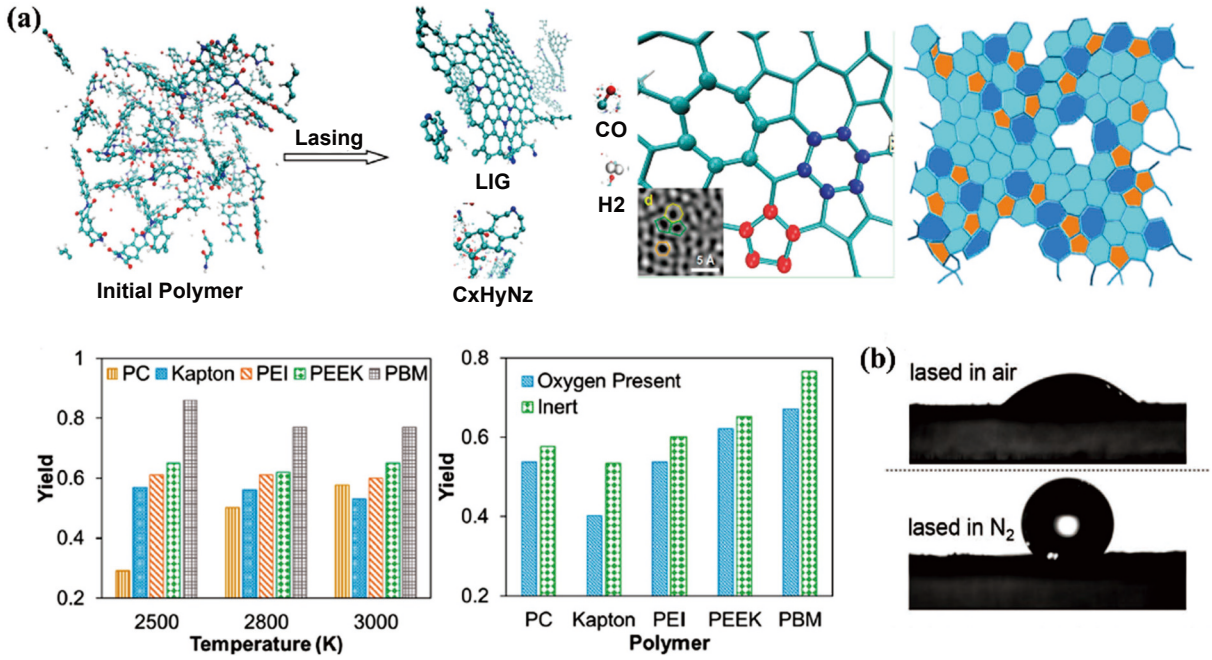

Fig. 2. (Color online) (a) Theoretical simulation of LIG synthesis process and the influence of temperature and oxygen on LIG production. Reproduced with permission from Ref. [29]. Copyright 2020, American Chemical Society. (b) Comparison of hydrophilicity of LIG produced in air and N_2 atmosphere. Reproduced with permission from Ref. [36]. Copyright 2021, Wiley-VCH.

garding the LIG technique are given and discussed. The possible schemes for improving the performance of LIG based devices are given, and the bright application prospects of LIG in practical devices are described.

2. Formation mechanism of LIG

Despite the high preparation speed of LIG, the mechanism is very complicated (i.e., a variety of reactions occur instantly). First, a high temperature generated by CO_2 laser is necessary, in addition to the atmosphere that will also affect the LIG formation. A widely accepted theory is that the laser causes high vibrations to propagate through the precursor material, which leads to local heating. This high energy is sufficient for bond dissociation of C–N, C–O, C–H and C=O bonds. During this photothermal conversion process, the material undergoes a transition from sp^3 to sp^2 hybrid state[12, 28]. To better understand this process, a ReaxFF reactive molecular dynamics simulation was carried out by Green (Fig. 2(a))[29]. The authors used polybenzimidazole (PBM), polyether ether ketone (PEEK), poly (ether imide) (PEI), polycarbonate (PC), and polyimide (Kapton) as research objects, because these polymers are proven to produce LIG[30]. The para-

meters were: atoms 1400, density 0.8 g/m^3, time step 0.25 fs, temperature 2000–4000 K. The result shows that the 2500–3000 K temperature range resulted in the best quality and yield of LIG, the LIG contains 5-, 6-, and 7-member carbon rings, which was caused by the rapid formation and cooling of the graphene, trapping it in a higher energy state. The spacing between the consecutive graphitic layers was found to be 3.4–4.0 Å. These simulation results match well with the experimental results.

During the high-temperature processing for LIG fabrication, the surface area increases with time. In the initial 0.2 ns at 3000 K, an amorphous structure is generated, which starts to transform to a more graphitic structure after ~0.2 ns. At the same time, small molecules dissociate from the polymer are released as gases along with $C_xH_yN_z$ species. CO and H_2 are two main gases in the LIG production, and the rate of evolution increases as simulation temperatures increase (between 2500–3000 K), in which Kapton produces the highest number of CO molecules because the monomer has the highest weight percentage of oxygen. The porosity of LIG is associated with the liberation of gas during the transformation process and a high laser power will increase the porosity[12].

The direct production of LIG from biomass polymers is challenging. Unlike the proven polymers that can be converted to LIG, polysaccharide chain biopolymers such as cellulose and chitosan are easily decomposed into levoglucosan, and are then further decomposed into volatile gases under the laser process with strong local heating[31]. Therefore, it is difficult for these biopolymers to generate graphene under laser induction. The coordination of metal ions is expected to play an important role in the formation of LIG from biopolymers[32]. For example, the addition of copper ions helps the chitosan film to retain solid carbon under the action of laser. This retention of solid carbon can provide necessary carbon as a precursor for the synthesis of graphene. In the transient high temperature process generated by the laser, the reduced Cu nanoparticles melt into their liquid form. The thermal movement and surface tension of the liquid copper atoms minimize their surface energy, thereby forming a defect free and smooth liquid copper surface[33]. This liquid copper surface enables carbon atoms to migrate rapidly and subsequently form graphene structures[33, 34]. Except for copper, some metals have higher carbon solubility after melting, resulting in the precipitation of additional carbon atoms from the surface of the liquid metal, which can promote the formation of a multilayer graphene structure[35].

Notably, the characteristics of M-LIG (metal-LIG) can be adjusted by controlling the laser parameters and the initial concentration of chelate metal ions in the biopolymer membranes, revealing its potential as a high-value M-LIG catalyst for a wide range of applications. Besides the laser parameters, the atmospheric environment also has an important influence on the formation of LIG. High O_2 content will decrease the LIG yield because of the drastic oxidation behavior, LIG produced at high O_2 atmosphere shows lower conductive and higher hydrophily. In contrast, LIG produced at N_2 atmosphere exhibits hydrophobic property (Fig. 2(b))[36]. Consequently, the LIG can be adjusted to different types by controlling laser parameters and atmosphere according to requirement, which is suitable for multifunctional applications.

3. Physical device applications

3.1. Flexible electronics

Point-of-care wearable devices are growing rapidly with functions to transform external stimuli into readable electrical signals. For the sensor components, stretchability and flexibility are the two important targets. Conventional metal-based strain sensors are rigid with low sensitivity and low flexibility, which fails to meet the demand for complex signal detection in the human body[37]. Therefore, to better improve the application scenarios of bioelectronics, soft materials with high conductivity are required as sensors, such as LIG.

It was previously proposed that LIG can be produced on many polymer surfaces, while some elastic-based LIGs are suitable for direct application without any treatment[5, 38]. Zhang's group found that a commercial CO_2 laser can directly engrave carbonized patterns on Kevlar clothes, and multiplecharacterizationsindicatedthattheblackcarbonisgraphene (Fig. 3(a))[5]. Due to the in-situ growth of graphene on the large area flexible substrate, they can be directly used as wearable devices to detect heart rate, or combined with zinc foil to construct a textile-based zinc-air battery as an energy source to drive other biosensors. Gas sensors are one of the most promising applications. The absolute value of the response to the sensor ($|\Delta R|/R_0$) increases monotonically from 0.33% to 4.02% with an increasing NO_2 concentration from 10 to 200 ppm, which shows good sensitivity. It is of great significant to integrate the NO_2 gas sensor on the clothes when used in laboratories and fires, and promptly remind the users of danger.

Clothes are very creative as a substrate for growing graphene, but in most cases, thin polymer films are used as a base material, because they are homogeneous, cheap and very suitable for mass produce. However, most polymer films, such as polyimide and lignin are not elastic. Therefore, additional steps are required to transfer LIG to the elastic substrate[27, 39–42]. Park *et al.* fabricated a temperature-strain hybrid sensor that exploits the outstanding properties of black phosphorus and LIG[43]. They firstly produced LIG on PI film, then transformed it with polystyrene-block-poly(ethylene-ran-butylene)-block-polystyrene (SEBS) substrate, and finally packaged it with SEBS by heat pressure (Fig. 3(b)). The device has both temperature and strain response with high sensitivity and duration, which can be used as a multifunctional sensor.

For flexible electronics, air permeability is increasingly becoming important, which is related to long-term wearing comfort (e.g., airtight devices can cause damage to the skin). Introducing porous structures into existing functional materials is a powerful way to tailor their gas permeability and other properties such as stretchability, modulus, and optical transmission[44, 45]. There are many elastomers including commercial tape that are air permeable, among which a sugar-templated elastomer sponge made by Yan *et al.* works well[46]. The authors transformed the graphene on PI to elastomer/sugar composites, and then dissolved sugar to get air-permeable flexible sensors. The sensor can be stretched to more than 600% of its original length with negligible resistance change, repeated more than 100 times, and is very suitable for wearable applications. Air permeability is the highlight of the

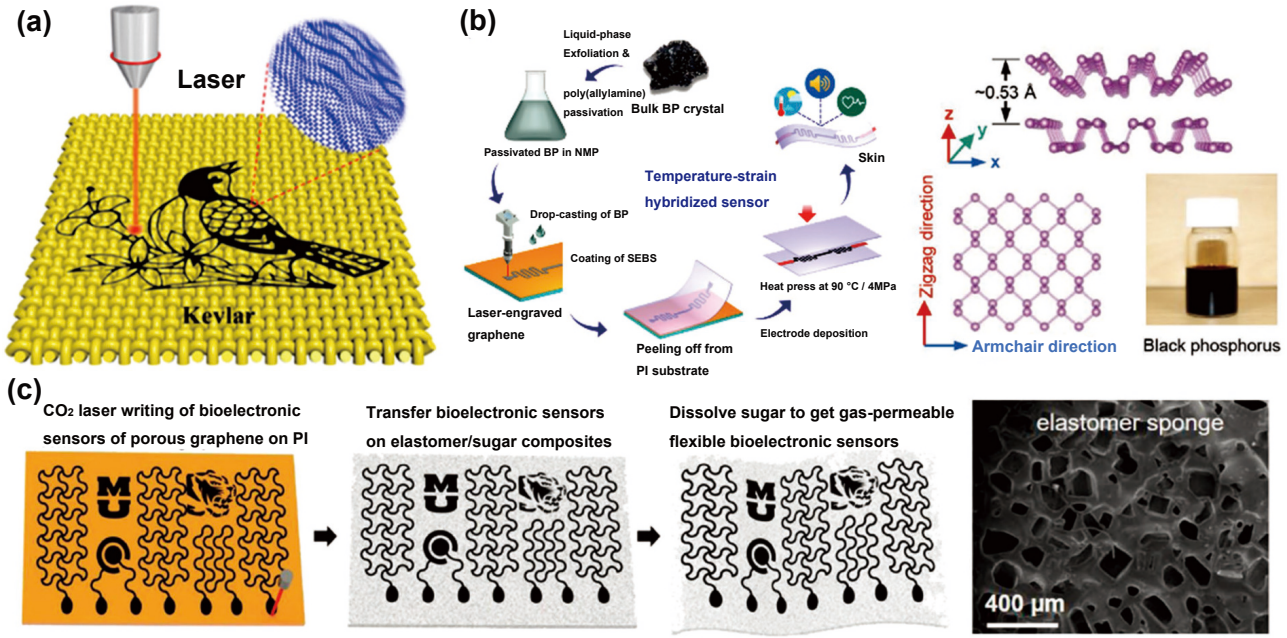

Fig. 3. (Color online) (a) Laser engraved carbonized patterns on Kevlar clothes. Reproduced with permission from Ref. [5]. Copyright 2020, American Chemical Society. (b) Temperature–strain hybrid sensor made by black phosphorus modified LIG. Reproduced with permission from Ref. [43]. Copyright 2020, Wiley-VCH. (c) High permeability stretch sensor based on elastic sponge. Reproduced with permission from Ref. [46]. Copyright 2018, Wiley-VCH.

sensor. In this research, the permeability of porous graphene on elastomer sponges is about 18 times higher than that of the elastomer substrates without pores (Fig. 3(c)).

Recently, an interesting application of LIG–soft robotics is demonstrated by Zheng *et al.*[47]. The authors glued LIG and PDMS of various shapes together, when a large current is applied, LIG and PDMS will undergo thermal expansion due to the Joule-heating effect of carbon. Because of the different moduli of LIG and PDMS, the planar 2D structure will be bent into a 3D structure when energized, and the 3D structure can be adjusted by the current and the modulus of PDMS. Furthermore, the authors demonstrated multiplied applications, including artificial muscles that can lift about 110 times their own weight, a biomimetic frog tongue that can prey insects, elastic metamaterials with human gestures-controlled bandgap behaviors, and a soft robotic finger that can measure ECG signals from human fingers in an on-demand and reversible manner.

3.2. Energy harvesting

Recently, carbon-based materials, such as graphene[48] and carbon nanotubes[49] have been used in triboelectric nanogenerators (TENGs), which can efficiently convert mechanical energy from the environment into electricity. As a new type of energy harvester, TENGs has the advantages of simple structure, portability, and high-power density, making them suitable for wearable power supplies. However, complex synthesis methods of carbon materials, such as spin coating or vacuum filtration, have limited their further application. Due to its ease of manufacture and high performance, LIG is very suitable for use as an electrode for triboelectric technology[50]. In addition, the widely used substrate PI can be directly used as an insulating layer, which simplifies the device.

A LIG/PI composite has been used to fabricate TENGs based on conductor-to-dielectric and metal-free dielectric-to-dielectric device geometries, the open-circuit voltages and peak powers exceeded 3.5 kV and 8 mW respectively[51]. Furthmore, LIG based TENGs can also be used in real life. When combining LIG and PDMS (highly tribonegative) into a flip-flop for electrical power generation on shoes and walking at a frequency of 2 Hz, the STENG can store electrical energy in a capacitor at a rate of ~2.4×10^{-2} mJ/s, demonstrating its potential as a portable power generator[52].

Some research work has found that the triboelectric effect of LIG varies greatly from different morphologies[25]. By changing the work distance of laser to cause defocus, the LIG morphology is modulated in porous LIG, in short carbon fiber combined LIG (SF-LIG) and in long carbon fiber-dominant LIG (LF-LIG). The results show that the LIG in the form of fibers has a slightly lower conductivity than the porous LIG, in which LF-LIG with graphitic N component can achieve better triboelectrification efficiency due to the lowered work function (Φ = 4.62 eV). Based on these advantages, the output performance of LF-LIG TENGs shows a power density of 512 mW/m^2, 130 times larger than the efficiency of the LIG TENGs, and the TENGs maintains its performance for ~10^4 cycles, which is sufficient to light up a hundred LEDs.

Recently, Zhao *et al.* proposed a new type of high-efficiency liquid–solid friction nanogenerator using super-hydrophobic fluorine-doped LIG[20]. They first dissolved the PI (colloid) in the N-methylpyrrolidone (NMP) solution. After spin coating on the substrate, the NMP solvent was removed to synthesize a 50 μm thick polyimide film. A fluorinated ethylene propylene (FEP) film (10 μm) was then coated by thermo-compression on the PI surface. Using picosecond UV laser to engrave F-doped LIG on the top of FEP-PI film and LIG on the back side of FEP-PI film, as shown in Fig. 4. The sandwich structure of the triboelectric nanogenerator exhibits a very high-power conversion efficiency. It can generate a peak power of 15.2 mW with the power density of 47.5 W/m^2 during the slid-

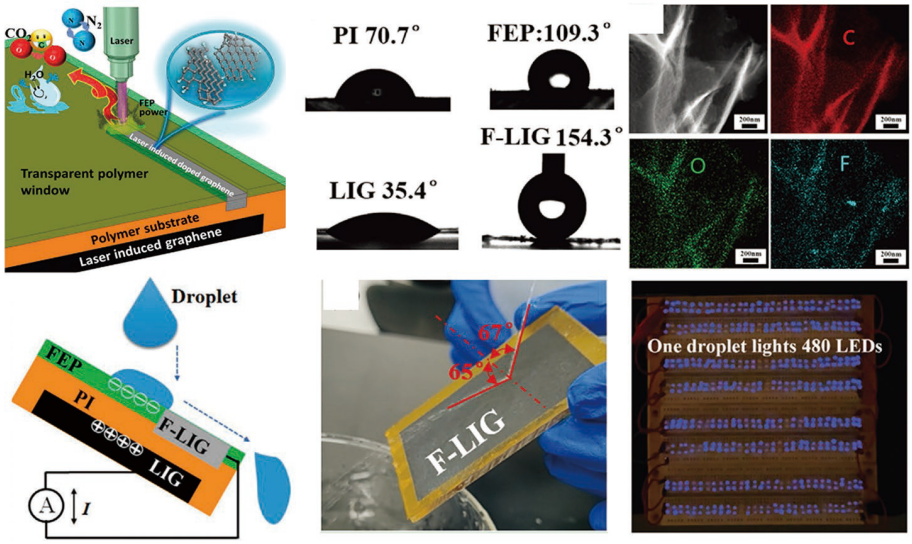

Fig. 4. (Color online) Liquid-solid friction nanogenerator using super-hydrophobic fluorine-doped LIG. Reproduced with permission from Ref. [20]. Copyright 2021, Wiley-VCH.

ing of one small water droplet with a volume of 105 μL from a height of 25 cm, and only one droplet can light 480 LEDs. More importantly, the operational stability of the device was also carefully studied under various harsh conditions. It can maintain 88% of the peak power at a high humidity level of 96% and 70% of the peak power density after 10 000 cycles, which is very robust and has great application prospect.

From this research work, we can conclude that LIG has a great potential for physical device applications. Among them, PI is the mostly used carbon source because of its low price and stable quality, along with good performances than many other carbon sources based LIG. For flexible electronics, the tensile property is one of the key goals. Consequently, it is essential to transform the LIG from PI substrate to other elastic substrates, such as PDMS and SEBS. Due to the strong Vander Waals force, soft carbon materials can bond with elastic substrates well and show stable performance. In TENGs, tensile properties are not required, and PI can be used as an insulating layer, so PI based LIG can be used directly in TENGs. The high-power density and portability make TENGs a very promising energy source and may be widely used in the future.

4. Chemical device applications

4.1. Biosensors

With the advent of intelligent life, chemical sensing is becoming ever more important to human health monitoring and regulation. Among them, various types of LIG-based sensors have been developed because of their special porous structure, large specific surface area and rich surface defects[52, 53]. Moreover, the fabrication of LIG based sensors is facile and cost-effective compared to the complicated lithography and other techniques, which leads to an extensive research area.

Dreimol *et al.* introduced iron catalyzed laser-induced graphitization (IC-LIG) as an innovative method for engraving large conductive graphene structures on wood with very high quality and efficiency, which overcomes the limitations of traditional LIG and can transform wood into a highly durable strain sensor. Their results pointed out the key role of iron in promoting the formation of highly conductive LIG, and revealed the structure property relationship of the obtained graded porous graphite like conductive foam[54]. Pristine LIG had been directly used to detect some small molecules[55–57], due to the ultra-large surface areas and surface defects generated during the laser engraving process along with the high electrical conductivity. For example, Gao's group explored a LIG-based sweat sensor for the simultaneous detection of uric acid (UA) and tyrosine (Tyr) by laser engraving and microfluidic design to realize the integration of sample collection and real-time detection[55]. Figs. 5(a) and 5(b) showed the scheme and mechanism of the three electrode LIG-based sensor in which UA and Tyr can be detected selectively based on the different oxidation potential. Furthermore, they demonstrated that the LIG-based sensors are superior to the conventional materials of glassy carbon (GCE), screen-printed carbon (SPE), and gold electrodes (AuE) for the chemicals analysis, as shown in Fig. 5(c).

In addition, LIG has also been developed to detect more specific chemicals through surface functionalization including ions like ammonium ions[59, 60], small molecules like glucose and hydrogen peroxide[61–65], pathogens like Escherichia coli[58, 66], SARS-CoV-2[67] and chloramphenicol[68] and so on. The principle of these sensors is usually based on the change of electrochemically capacitance, impedance or potential caused by chemicals adsorption of LIG[69]. The modified materials generally involve metal/metal oxide nanoparticles, ionophores, molecular polymer, and antibodies[64, 70–72]. For instance, You *et al.* reported an AuNPs/LIG based impedimetric immunosensor modified by corresponding antibody for the detection of pathogen O157:H7, as schematically illustrated in Fig. 5(d)[58]. With the synergistic effect of LIG and Au nanoparticles together with the specific antibody, the integrated immunosensor exhibited excellent performance with low detection limit and high selectivity for Escherichia coli O157:H7 (Figs. 5(e)–5(g))[58]. Recently, our group reported a new strategy to engineer the LIG surface with Au clusters and chitosan sequentially to form a C–Au–LIG electrode with a superhydrophilic and highly conductive 3D graphene surface, which demonstrates superior performance and negligible decay in both long-term storage and practical usage in vitro and in vivo environments. This wearable biosensor based on

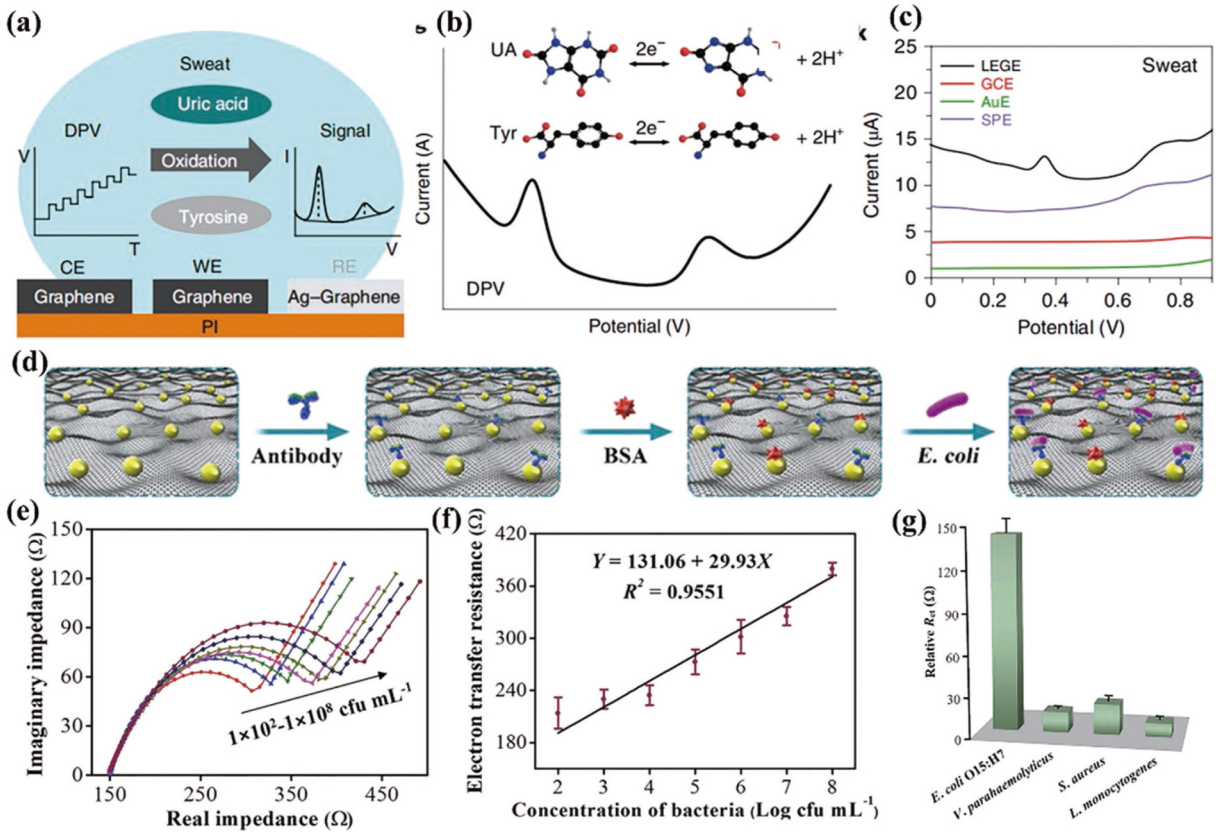

Fig. 5. (Color online) (a) Diagram of a three-electrode sweat UA and Tyr sensors. (b) The different oxidation peak height for the detection of UA and Tyr. (c) Detected signals in the raw sweat samples measured by different electrodes. Reproduced with permission from Ref. [55]. Copyright 2020, Nature Research. (d–g) Schematic illustration, performance, and specificity of the AuNPs/LIG based immunosensor for the detection of Escherichia coli O157:H7. Reproduced with permission from Ref. [58]. Copyright 2020, Elsevier Ltd.

the C–Au–LIG electrode that can detect uric acid and pH simultaneously with negligible decay for more than one month, which shows a potential application prospect (Fig. 6)[23].

4.2. Supercapacitors

Supercapacitors (SCs) possess advantages of high power density, fast charge/discharge rates, and long-term cyclability, and have been applied to automobiles and other fields[73]. Basically symmetrical porous carbon-based electrodes are used in most SC, which benefit from their high porosity for the electrolyte reservoir and large specific surface areas for the ion adsorption[74]. LIG is a porous carbon material with similar merit and simple synthesis, and is suitable for SC, while the low energy densities mainly and largely prevent the extensive applications of SC[75, 76]. At present, there are three main tactics to overcome this shortcoming, namely control of surface structures, coupling with pseudocapacitive materials, and design of hybrid devices[77].

The advantages of laser scribing are helpful to regulate the structure of electrode material and utilize the effect of structure-activity correlation efficiently. Kaner *et al.* found that the specific surface area of GO can be increased to 1520 m^2/g with excellent electrical conductivity of 1738 S/m after laser scribing, which endow the superior electrochemical performance[78]. The further enhanced performance have been realized through the introduction of N or B heteroatoms[75, 79]. The NB-LIG with 1 wt% H_3BO_3 obtained 2.5 and 12 times improvement in specific areal capacitance at 0.2 mA/cm^2 compared to the N-LIG and undoped LIG, respectively[75]. As shown in Figs. 7(a)–7(c), the densified and well-balanced porous structure resulting from the laser-etched microchannels facilitated the diffusion of ions at the electrode/electrolyte interface along with the synergistic effect of N and B co-doping, which enhanced the capacitive performance.

Besides directly using as carbon electrodes for SC, these laser-enabled porous LIGs have also served as excellent substrates for loading pseudocapacitive materials. Up to now, nanostructured MnO_2, Fe_3O_4, MoS_2, and conductive polymer, for example, had been hybridized with the laser-derived porous carbon framework to effectively utilize pseudocapacitive energy[22, 80, 81]. One hopeful advantage of this kind of electrode is the retention of excellent performance even with ultra-thick electrodes. For instance, the carbon-loaded MnO_2 electrodes as thick as 110 mm could still perform an extremely large specific capacitance. The perpendicularly oriented graphene nanosheets, which allow a long electron transfer path along vertical direction, are primarily responsible for this extraordinary performance. Another recent promising example was the solvothermal growth of conductive MOF nanorods on LIG substrates, which offered rapid redox activity in both positive and negative potential ranges (Fig. 7(d))[82]. As a result, a symmetric pseudocapacitive capacitor with a large voltage window was constructed on these electrodes, as revealed in Fig. 7(e).

The design of hybrid SC can also be implemented easily by laser engraving with the assistance of programmable processing for a series and parallel connections of multiple devices, rendering dynamic energy output[85, 86]. For example,

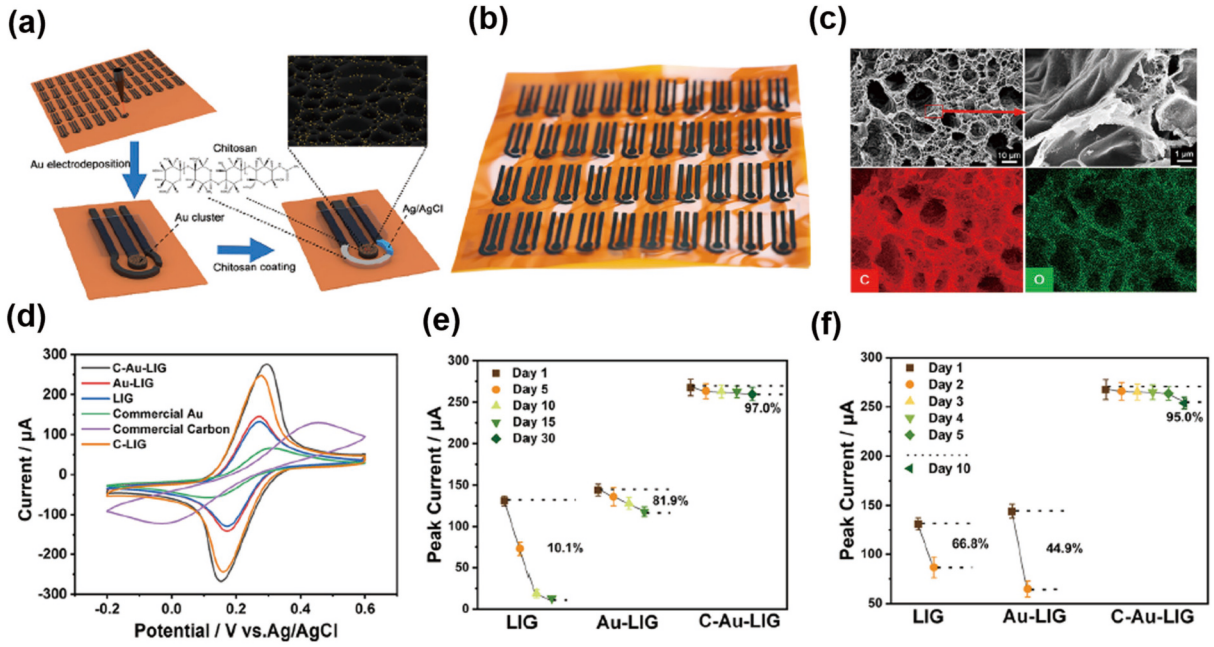

Fig. 6. (Color online) (a–c) Schematic diagram of the C–Au–LIG fabrication process and related SEM images. (d) Representative CV curves of different biosensors in standard potassium ferricyanide solution. (e) Redox peak currents of LIG, Au–LIG, and C–Au–LIG after different periods of time in ambient environments. (f) Redox peak currents of LIG, Au–LIG, and C–Au–LIG in continuous usage. Adapted with permission from Ref. [23]. Copyright 2022, American Chemical Society.

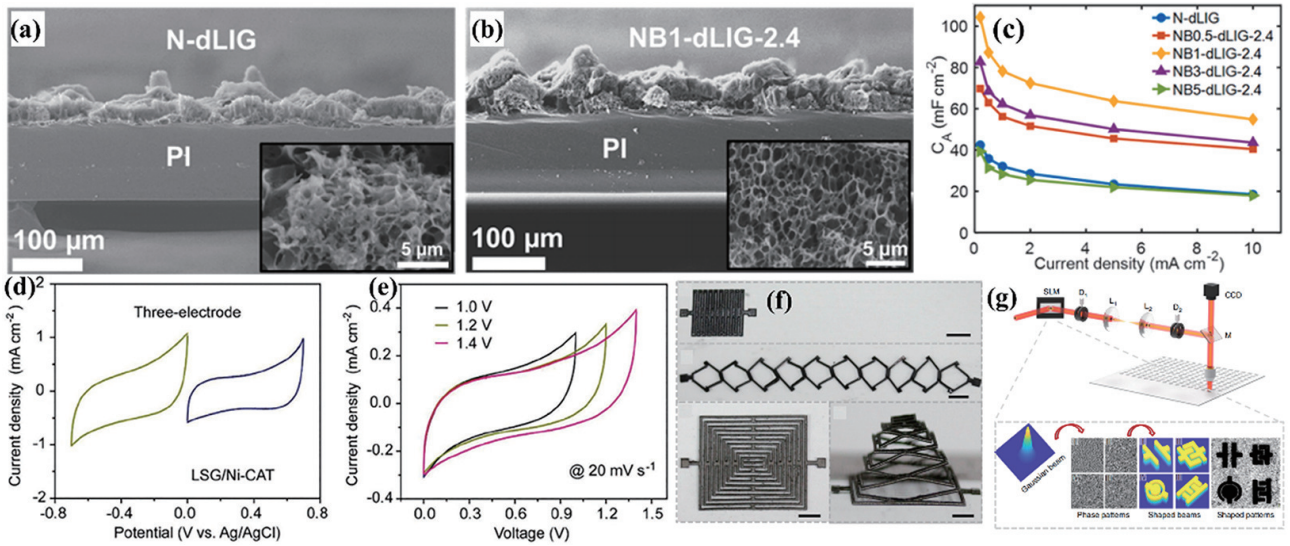

Fig. 7. (Color online) (a–c) SEM images and the areal specific capacitance of doping LIG. Reproduced with permission from Ref. [75]. Copyright 2022, Elsevier Ltd. (d, e) Electrochemical performance of conductive MOF-derived LIG. Reproduced with permission from Ref. [82]. Copyright 2019, Wiley-VCH. (f) Illustration of customer-designed supercapacitors enabled by laser irradiation. Reproduced with permission from Ref. [83]. Copyright 2019, American Chemical Society. (g) Gaussian beams were transformed into arbitrary geometric target beams by programming phase patterns for the synthesis of different SC. Reproduced with permission from Ref. [84]. Copyright 2020, Nature Research.

Gao *et al.* enlightened by the stereo paper cutting idea proposed a laser direct writing strategy for fabricating multi-dimensional SC based on the large planar graphene-based SC, while the garland configuration allowed the SC to be stably operated even at a 5-fold stretching, suggesting an alternative approach to constructing flexible energy storage devices, as shown in Fig. 7(f)[83] . In addition, Yuan *et al.* reported an ultrafast method to prepare various and large-scale patterning LIG based SCs by real one-step femtosecond laser irradiation. They converted the Gaussian beam to various beam shapes via phase modulation to provide a spatially-shaped femtosecond laser source (Fig. 7(g))[84]. Therefore, more comprehensive technology of laser preparation for different industrial needs will inevitably be developed.

4.3. Rechargeable batteries

Rechargeable batteries play an important role in energy storage and conversion, which can repeatedly produce stable power output mainly through the reversible redox of different materials to achieve stable charge and discharge. With the application and development of rechargeable batteries, there are now not only lithium ion batteries (LIBs) with in-depth study but also sodium-ion batteries (SIBs), lithium-met-

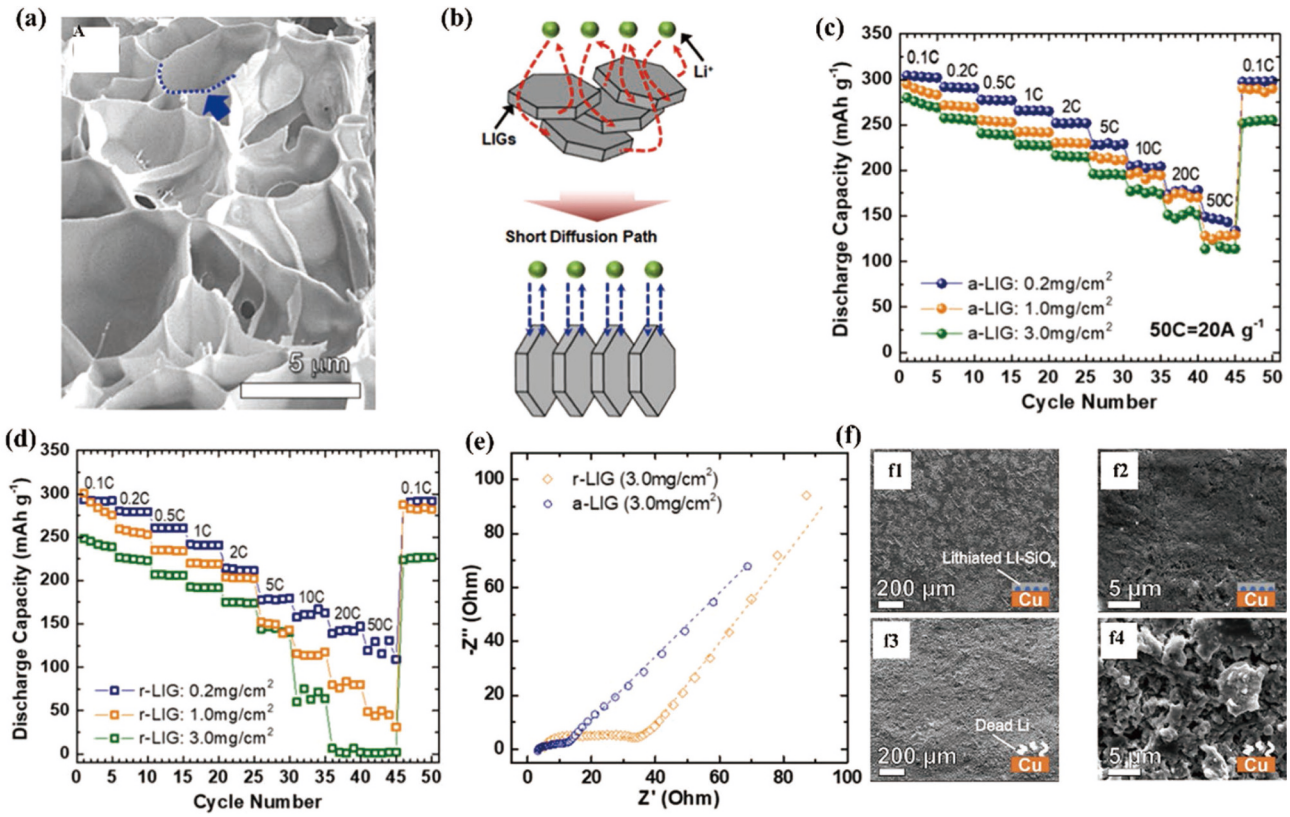

Fig. 8. (Color online) (a) SEM image, (b) schematic illustration of Li diffusion path, and (c–e) electrochemical performances of a-LIG. Reproduced with permission from Ref. [91]. Copyright 2021, Elsevier Ltd. (f) SEM images of Cu-$LiFePO_4$ full cell after 50 cycles with LI-SiO_x coating or not. Reproduced with permission from Ref. [93]. Copyright 2020, Wiley-VCH.

al batteries (LMBs), aqueous zinc-ion batteries (ZIBs), and so on.[87, 88]. Compared to supercapacitors, the batteries possess higher energy densities due to the phase conversion of electrode material, but sluggish reaction kinetics and poor long-term safety impair their performance. At present, the performance of the batteries can be further optimized through rationally designing the composition and structure of electrode materials to improve the ion transport and inhibit the dendrite growth[89, 90]. High specific surface area and simple preparation of LIG make it attract the attention of scientists to get these two improvements mentioned above.

There is a growing need for fast charging/discharging LIBs, which depend on the intrinsic properties of the electrode material and the surrounding environment, such as structural engineering for the improvement of ionic transport. Shim *et al*. fabricated a facet-controlled 3D holey graphene as high-rate anode material by transferring LIG onto a Cu current collector[91]. This electrode exhibited fast charging/discharging property for charging 95% capacity of ~114 mAh/g within 3 min at a mass loading of 3 mg/cm^2, which is attributed to the hierarchical 3D holey structure of the transferred LIG (a-LIG). In contrast to the randomly stacked LIG (r-LIG), the rate performance indicated that the facet-oriented surface of a-LIG with abundant graphitic edges was more conducive to the fast Li ion transport, due to its shorter diffusion path and smaller internal resistance (Figs. 8(a)–8(e)). In addition, Zhang *et al*. reported an N-doped porous graphene anode directly on Cu foil via a single-step laser-based transformation of urea-containing polyimide, which take better advantage of the simplicity of LIG. These 3D LIG structures perform inordinately well as anodes for SIBs with excellent rate capabilities and initial coulombic efficiency of approximate 74% preceding most reported carbonaceous anodes[92].

The long-term safety of batteries is particularly essential, so it is necessary to improve the problem of dendrite growth, which causes irreversible capacity loss and may puncture the diaphragm leading to overheating or even spontaneous combustion. Tour *et al*. synthesized a laser-induced silicon oxide (LI-SiO_x) layer with a small amount of LIG generated from a commercial PI adhesive tape on Cu current collector to optimize the reversibility of LMBs[93]. The laser-induced coating resulted in a superior performance by suppressing the formation of Li dendrites and inactive Li compared to the bare electrodes, as shown in (Fig. 8(f)). In the process of Li deposition, the small amount of LIGs serve as uniform nucleation sites during the initial plating process combined with lithiophilic nature of LI-Si-O_x, which make the coated Cu possess more favorable nucleation kinetics. This similar strategy was developed to ZIBs by Guo et al. by preparing zincophilic LIG interlayer for homogenous Zn deposition[94].

4.4. Electrocatalysis

Electrocatalysis is a catalytic process that accelerates charge transfer at the electrode and electrolyte interface. At present, a great deal of attention has been paid to some catalytic reactions, such as hydrogen evolution reaction (HER), oxygen evolution reaction (OER), oxygen reduction reaction (ORR) and carbon dioxide reduction reaction (CO_2RR), which are essential components of energy conversion process[19, 95]. Generally, these reactions are kinetically tardy and therefore require highly active electrocatalysts to facilitate them. The re-

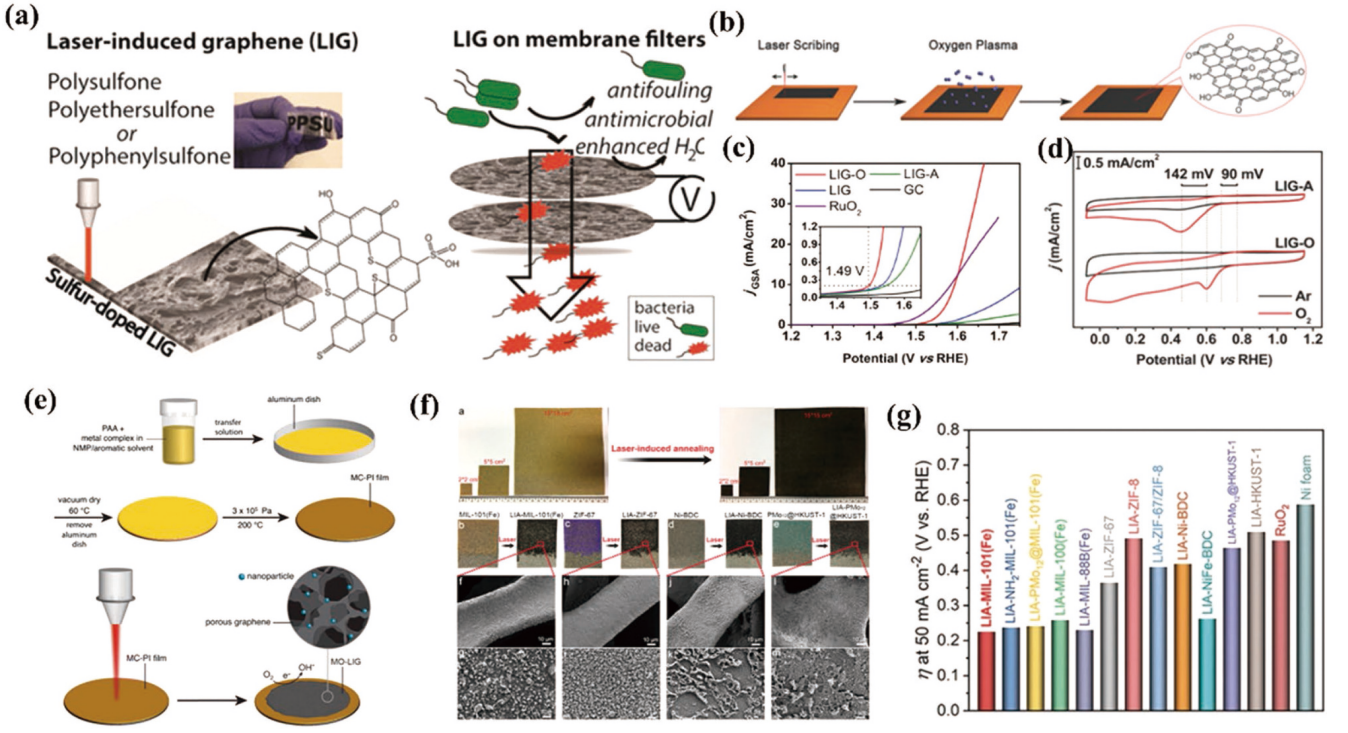

Fig. 9. (Color online) (a) Schematic illustration of the synthesis and the electrochemical ORR and antifouling along with antimicrobial properties of S-LIG. Reproduced with permission from Ref. [96]. Copyright 2018, American Chemical Society. (b) Preparation and (c, d) electrochemical performance of LIG-O. Reproduced with permission from Ref. [97]. Copyright 2018, Wiley-VCH. (e) Schematic illustration of formation of MO-LIG from MC-PI film. Reproduced with permission from Ref. [98]. Copyright 2015, American Chemical Society. (f) Photographs and SEM images of different MOF-derived LIG. (g) Comparation of overpotentials for 50 mA/cm^2. Reproduced with permission from Ref. [99]. Copyright 2021, Wiley-VCH.

search on electrocatalyst about LIG produced by simple and efficient methods abounds because of its high specific surface area and excellent electroconductivity[69]. LIG can be used as electrocatalyst directly through in-situ synthesis or as a carrier of other active substances for collaborative catalysis.

Through the introduction and doping of heteroatoms which can change the electronic structure to improve the activity, LIG has been used as a direct active catalyst without metal. Singh *et al.* reported a laser-induced synthesis of sulfur-doped porous LIG (S-LIG) using sulfur-containing polymer membranes, such as polyphenylsulfone for catalytic H_2O_2 generation in ORR and antifouling application (Fig. 9(a))[96]. The authors showed that the initial antifouling properties are derived from the improved hydrophilicity and surface charge of S-LIG due to the doped S element so as to prevent the attachment to organic pollutants and bacteria. The antimicrobial performance can be further improved by electrochemical catalysis with a voltage bias to generate H_2O_2. In addition, Zhang *et al.* exhibited that the oxidation of LIG (LIG-O) via O_2 plasma can promote the catalytic activity of OER and ORR (Figs. 9(b)–9(d)). The oxygen-containing groups in the LIG-O not only provided the extra active sites, but also boost the adsorption of reactive intermediates and reduced the reaction activation energy[97].

Due to the high surface area and conductivity of graphene, coupled with the free-standing characteristics of normal LIG, LIG has been studied extensively as an outstanding substrate for the preparation of a 3D integrated catalytic electrode[13, 69]. Transition metal-based catalysts have become a hot topic in replacing noble metal-based electrocatalysts because of their good performance and low cost. Tour's group developed a method for ex-situ or in-situ synthesis of porous graphene catalysts embedded with metal (oxide) nanoparticles after simple introduction of metal precursor[98, 100–103]. For example, they prepared the NiFe/LIG catalysts by loading the metal ion solution onto a prefabricated LIG via PI film and laser scribing again. This method avoided traditional complex solution-based reactions by laser-guided solid phase transformation. The NiFe/LIG showed excellent OER performance with an overpotential (10 mA/cm^2) of 240 mV and a Tafel slope of 32.8 mV/dec in alkaline electrolyte as normal NiFe-based catalyst[100]. In addition, this group optimized the above method needing two-time laser scribe by adding metal-complex to form metal-complex-containing PI film (Fig. 9(e)) and even using biodegradable cedar wood which soaked metal salt solution as precursor. These metal-salt-containing precursors were transformed in-situ to metal or metal oxide nanoparticles embedded in porous graphene after one-step simple CO_2 laser scribing, and these materials showed great ORR or OER performance[98, 103]. Tang *et al.* reported a precise laser-induced annealing approach with MOFs as the precursor (Fig. 9(f)), which improved the conventional thermal transition of MOFs to electrocatalysts and avoided severe aggregation of metal particles. Remarkably, as prepared LIA-MIL-101(Fe) on nickel foam displays an ultralow overpotential of 225 mV to reach 50 mA/cm^2 and wonderful durability beyond 50 h for promoting the OER, exceeding most reported transition-metal-based materials and benchmark RuO_2 catalysts (Fig. 9(g))[99].

Other classical methods for loading active materials have

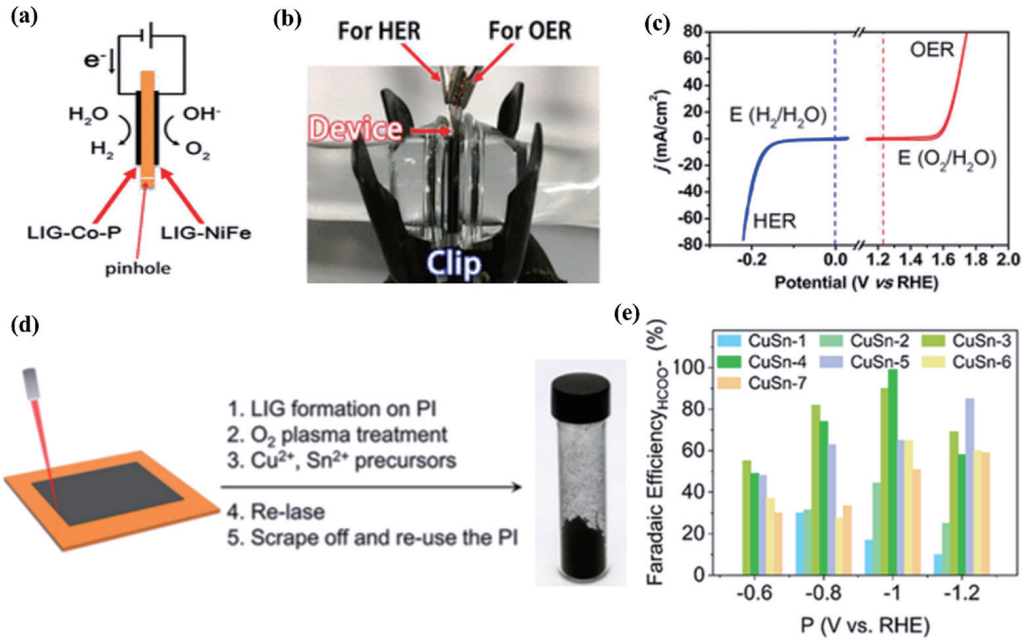

Fig. 10. (Color online) (a–c) A full water-splitting device made by laser irradiation followed by electrodeposition and its performance. Reproduced with permission from Ref. [104]. Copyright 2017, American Chemical Society. (d) Preparation and (e) CO_2RR performance of the CuSn-LIG catalysts. Reproduced with permission from Ref. [105]. Copyright 2020, American Chemical Society.

been combined to synthesize highly efficient composites electrode based on LIG. Nayak *et al.* fabricated a 3D graphitic carbon substrate loaded with Pt via laser scribing of PI film and further atomic layer deposition (ALD) of Pt for boosting HER[106]. The cooperative effects between the Pt of ALD and the 3D LIG provided an approach to efficiently use noble metals and give as much exposure to active sites as possible resulting to an improved HER activity. The 3D LIG with good conductivity and numerous plane-edge active sites makes it possible to synthesize an integrated electrocatalyst without any agglomerants or other conductive additives. Moreover, electrodeposition is a simple, efficient, and low-cost method that has become an important tool to load active materials. Tour's group reported some relevant researches based on LIG and normal electrocatalysts including CoP and NiFe[104]. Thereinto *et al.* designed and prepared a novel integrated membrane electrode by laser carbonization and electrodeposition of catalytic materials on the both sides of plastic film, which simplified the manufacture of water electrolyzer for HER and OER (Figs. 10(a)–10(c))[104].

There has been some research on LIG-based electrocatalysts for water splitting and fuel cell covering the HER, OER, and ORR. Ren *et al.* shifted their attention to the CO_2RR, which is rarely studied. They reported a bimetallic CuSn-based catalyst to reduce CO_2 to formic acid by optimizing the ratio of Cu to Sn easily before laser scribing to achieve the optimal selectivity (Fig. 10(d)). The CuSn-4 with Cu/Sn atomic ratio close to 1 : 2 shows a faradaic efficiency of 99% for formic acid with a high partial current density of 26 mA/cm^2 (Fig. 10(e))[105]. For CO_2RR, some emerging technologies can also be combined with laser technology to achieve greater application value. For example, Hu's group reported a chitosan-based anionic conductor in which ion-conducting nanochannels were formed by crosslinking chitosan molecular chains with Cu^{2+} ions[107]. The chelated Cu^{2+} ions in chitosan-Cu selectively promote the transport of anions (OH^-) within the nanochannels, with a high hydrogen oxide conductivity of 67 mS/cm at room temperature. Cu^{2+} crosslinking also inhibited the swelling of the membrane in water, inhibited the fuel penetration and improved the mechanical strength. Subsequently, they coated chitosan-Cu HEM (hydroxide exchange membrane) with a cathode catalyst and sandwiched HEM between the anode electrode and the gas diffusion layer to form a membrane electrode assembly (MEA) for DMFC (direct methanol fuel cell). The excellent performance of DMFC verifies the excellent conductivity and unique structural advantages of chitosan copper membrane as an ion exchange membrane for fuel cells. Thus, the chitosan-Cu anion exchange membrane will show application prospects for CO_2RR. If the method of coating catalyst on cathode is changed to the method of direct laser printing on HEM, an integrated electrode with high current density and high stability will be prepared. It is believed that more related work based on LIG will appear in the future, involving laser adjustment of crystal structure, defects and hydrophilicity for CO_2RR, as well as active site design based on membrane and metal material precursors, and even other important electrocatalytic reactions.

The main advantage of LIG in chemical device applications is their high specific surface area. In liquid phase, high specific surface area means high electron exchange rate, so porous LIG with high conductivity exhibits high performance in applications that emphasize performance per unit geometric area, such as supercapacitors, rechargeable batteries, and electrocatalysis. In biosensors, graphene and Au are the two main sensor materials because of their stable properties and also because they are biologically friendly. However, graphene is more widely used in detecting biomarkers with redox properties (e.g., uric acid, and some sweat) or plasma included biomarkers (e.g., glucose, cortisol etc.) can also be detected by graphene after modification with enzyme or antibodies.

5. Summary and perspective

Here, we summarized the latest developments of LIG based device applications in both chemical and physical fields. The laser writing method can promote the rapid preparation of 3D porous LIG and accuracy control the porosity, composition, shape, and conductivity. Due to the easy fabrication process and multi-faceted performance, LIG based devices exhibited an obvious superiority over other graphene-based devices in many fields[55, 108] and their applications are still expanding. Flexible electronics are an early and most pertinent application of LIG because a single laser processing can be used for patterning, conductivity tuning, and circuit wiring at the same time, which significantly facilitates fabrication and assembly. LIG TENGs have recently been developed that can simplify the TENGs fabrication process due to the in-site growth on the PI, and to solve the difficulty of adhesion stability between conductive materials and PI substrate[51]. For chemical device applications, the high specific surface area, biocompatibility, and conductivity of LIG makes it potentially useful in the fields of the supercapacitors, electrocatalysis, and biosensors.

There is, however, still room to improve the performance of different LIG-based devices. For example, the packaging area of flexible electronics is still too large. To further improve the integration and resolution of interdigital electrodes, advanced femtosecond laser processing may be a good method[84]. For biosensor devices, because real-time monitoring of body signals is the future direction of human healthcare, the integration of multifunctional components on a single substrate to form self-powered "all-in-one" biosensors will be a very promising direction. For most other chemical devices, the single carbon material is not suitable for efficiently electrocatalytic water splitting and CO_2 reduction, as well as supercapacitors. Combining with other materials, such as Cu (for CO_2 reduction) and MnO_2 (for supercapacitors), is a useful strategy to future improve their performance. Of course, the combination of laser technology and biopolymer will also create new application scenarios, which are extremely attractive to the development of biology, environment, energy, and related fields. Overall, by keep improving the quality of LIG and their composites with advanced strategies, LIG will have a bright future for practical device applications in many fields.

Acknowledgements

This work was financially supported by the National Natural Science Foundation of China (NSFC, 52003225), Open Fund of Jiangsu Key Laboratory of Nano Devices (21SZ01).

References

[1] Song Y, Zou W, Lu Q, et al. Graphene transfer: Paving the road for applications of chemical vapor deposition graphene. Small, 2021, 17, 2007600

[2] Nair R R, Blake P, Grigorenko A N, et al. Universal dynamic conductivity and quantized visible opacity of suspended graphene. Science, 2008, 320, 1308

[3] Han J, Johnson I, Chen M. 3D continuously porous graphene for energy applications. Adv Mater, 2022, 34, 2108750

[4] Johnson Z T, Williams K, Chen B, et al. Electrochemical sensing of neonicotinoids using laser-induced graphene. ACS Sens, 2021, 6, 3063

[5] Wang H, Wang H, Wang Y, et al. Laser writing of janus graphene/kevlar textile for intelligent protective clothing. ACS Nano, 2020, 14, 3219

[6] Fei L, Choi K S, Park T J, et al. Graphene-based electrochemical biosensor for pathogenic virus detection. BioChip J, 2011, 5, 123

[7] Yagati A K, Behrent A, Beck S, et al. Laser-induced graphene interdigitated electrodes for label-free or nanolabel-enhanced highly sensitive capacitive aptamer-based biosensors. Biosens Bioelectron, 2020, 164, 112272

[8] Martinez A, Fuse K, Yamashita S, et al. Mechanical exfoliation of graphene for the passive mode-locking of fiber lasers. Appl Phys Lett, 2011, 99, 3077

[9] Guo J, Mao B, Li J, et al. Rethinking the reaction pathways of chemical reduction of graphene oxide. Carbon, 2021, 171, 963

[10] Blaha M, Bousa M, Vales V, et al. Two-dimensional CVD-graphene/polyaniline supercapacitors: synthesis strategy and electrochemical operation. ACS Appl Mater Interfaces, 2021, 13, 34686

[11] Tian B, Li J, Chen M, et al. Synthesis of AAB-stacked single-crystal graphene/hBN/graphene trilayer van der Waals heterostructures by in situ CVD. Adv Sci, 2022, 9, 2201324

[12] Jian L, Peng Z, Liu Y, et al. Laser-induced porous graphene films from commercial polymers. Nat Commun, 2014, 5, 5714

[13] Ye R, Chyan Y, Zhang J, et al. Laser-induced graphene formation on wood. Adv Mater, 2017, 29, 1702211

[14] Kothuru A, Goel S. Laser induced graphene on phenolic resin and alcohol composite sheet for flexible electronics applications. Flex Print Electron, 2020, 5, 042001

[15] Cho E C, Chang-Jian C W, Syu W L, et al. PEDOT-modified laser-scribed graphene films as bginder- and metallic current collector–free electrodes for large-sized supercapacitors. Appl Surf Sci, 2020, 518, 146193

[16] Nayak P, Kurra N, Xia C, et al. Highly efficient laser scribed graphene electrodes for on-chip electrochemical sensing applications. Adv Electron Mater, 2016, 2, 1600185

[17] You R, Liu Y Q, Hao Y L, et al. Laser fabrication of graphene-based flexible electronics. Adv Mater, 2020, 32, 1901981

[18] Kaidarova A, Kosel J. Physical sensors based on laser-induced graphene: A review. IEEE Sens J, 2021, 21, 12426

[19] Hu H, Li Q, Li L, et al. Laser irradiation of electrode materials for energy storage and conversion. Matter, 2020, 3, 95

[20] Chen Y, Xie B, Long J, et al. Interfacial laser-induced graphene enabling high-performance liquid-solid triboelectric nanogenerator. Adv Mater, 2021, 33, 2104290

[21] Rauf S, Lahcen A A, Aljedaibi A, et al. Gold nanostructured laser-scribed graphene: A new electrochemical biosensing platform for potential point-of-care testing of disease biomarkers. Biosens Bioelectron, 2021, 180, 113116

[22] Li L, Zhang J, Peng Z, et al. High-performance pseudocapacitive microsupercapacitors from laser-induced graphene. Adv Mater, 2016, 28, 838

[23] Zhang L, Wang L, Li J, et al. Surface engineering of laser-induced graphene enables long-term monitoring of on-body uric acid and pH simultaneously. Nano Lett, 2022, 22, 5451

[24] Cao L, Zhu S, Pan B, et al. Stable and durable laser-induced graphene patterns embedded in polymer substrates. Carbon, 2020, 163, 85

[25] Choi K H, Park S, Hyeong S K, et al. Triboelectric effect of surface morphology controlled laser induced graphene. J Mater Chem A, 2020, 8, 19822

[26] Kun H, Bin L, Orban M, et al. Accurate flexible temperature sensor based on laser-induced graphene material. Shock Vib, 2021, 2021, 1

[27] Dallinger A, Keller K, Fitzek H, et al. Stretchable and skin-conformable conductors based on polyurethane/laser-induced graphene. ACS Appl Mater Interfaces, 2020, 12, 19855

[28] Dreyfus R W. CN temperatures above laser ablated polyimide. Appl Phys A, 1992, 55, 335
[29] Vashisth A, Kowalik M, Gerringer J C, et al. ReaxFF simulations of laser-induced graphene (LIG) formation for multifunctional polymer nanocomposites. ACS Appl Nano Mater, 2020, 3, 1881
[30] Chyan Y, Ye R, Li Y, et al. Laser-induced graphene by multiple lasing: toward electronics on cloth, paper, and food. ACS Nano, 2018, 12, 2176
[31] Lee S, Jeon S. Laser-induced graphitization of cellulose nanofiber substrates under ambient conditions. ACS Sustain Chem Eng, 2019, 7, 2270
[32] Bergsman D S, Getachew B A, Cooper C B, et al. Preserving nanoscale features in polymers during laser induced graphene formation using sequential infiltration synthesis. Nat Commun, 2020, 11, 3636
[33] Tan L, Zeng M, Zhang T, et al. Design of catalytic substrates for uniform graphene films: from solid-metal to liquid-metal. Nanoscale, 2015, 7, 9105
[34] Kresse G, Hafner J. Ab initio molecular dynamics for liquid metals. Phys Rev B, 1993, 47, 558
[35] Li X, Cai W, An J, et al. Large-area synthesis of high-quality and uniform graphene films on copper foils. Science, 2009, 324, 1312
[36] Huang L, Gu M, Wang Z, et al. Highly efficient and rapid inactivation of coronavirus on non-metal hydrophobic laser-induced graphene in mild conditions. Adv Funct Mater, 2021, 31, 2101195
[37] Wang S, Kang Y, Wang L, et al. Organic/inorganic hybrid sensors: a review. Sens Actuat B, 2013, 182, 467
[38] Liu W, Huang Y, Peng Y, et al. Stable wearable strain sensors on textiles by direct laser writing of graphene. ACS Appl Nano Mater, 2020, 3, 283
[39] Li J T, Stanford M G, Chen W, et al. Laminated laser-induced graphene composites. ACS Nano, 2020, 14, 7911
[40] Rahimi R, Ochoa M, Yu W, et al. Highly stretchable and sensitive unidirectional strain sensor via laser carbonization. ACS Appl Mater Interfaces, 2015, 7, 4463
[41] Tian Q, Yan W, Li Y, et al. Bean pod-inspired ultrasensitive and self-healing pressure sensor based on laser-induced graphene and polystyrene microsphere sandwiched structure. ACS Appl Mater Interfaces, 2020, 12, 9710
[42] Wu Y, Beker L, Karakurt I, et al. High resolution flexible strain sensors for biological signal measurements. 19th International Conference on Solid-State Sensors, Actuators and Microsystems (TRANSDUCERS), 2017, 1144
[43] Chhetry A, Sharma S, Barman S C, et al. Black phosphorus@laser-engraved graphene heterostructure-based temperature-strain hybridized sensor for electronic-skin applications. Adv Funct Mater, 2020, 31, 2170068
[44] Cai L, Song A Y, Wu P, et al. Warming up human body by nanoporous metallized polyethylene textile. Nat Commun, 2017, 8, 496
[45] Pan F, Chen S M, Li Y, et al. 3D graphene films enable simultaneously high sensitivity and large stretchability for strain sensors. Adv Funct Mater, 2018, 28, 1803221
[46] Sun B, McCay R N, Goswami S, et al. Gas-permeable, multifunctional on-skin electronics based on laser-induced porous graphene and sugar-templated elastomer sponges. Adv Mater, 2018, 30, 1804327
[47] Ling Y, Pang W, Li X, et al. Laser-induced graphene for electrothermally controlled, mechanically guided, 3D assembly and human-soft actuators interaction. Adv Mater, 2020, 32, 1908475
[48] Xia X, Chen J, Liu G, et al. Aligning graphene sheets in PDMS for improving output performance of triboelectric nanogenerator. Carbon, 2017, 111, 569
[49] Hwang H Y, Lee K Y, Shin D G, et al. Metal-free, flexible triboelectric generator based on MWCNT mesh film and PDMS layers. Appl Surf Sci, 2018, 442, 693
[50] Yan Z, Wang L, Xia Y, et al. Flexible high-resolution triboelectric sensor array based on patterned laser-induced graphene for self-powered real-time tactile sensing. Adv Funct Mater, 2021, 31, 2100709
[51] Stanford M G, Li J T, Chyan Y, et al. Laser-induced graphene triboelectric nanogenerators. ACS Nano, 2019, 13, 7166
[52] Tao L Q, Tian H, Liu Y, et al. An intelligent artificial throat with sound-sensing ability based on laser induced graphene. Nat Commun, 2017, 8, 14579
[53] Zhang C, Xie Y, Deng H, et al. Monolithic and flexible ZnS/SnO_2 ultraviolet photodetectors with lateral graphene electrodes. Small, 2017, 13, 1604197
[54] Dreimol C H, Guo H, Ritter M, et al. Sustainable wood electronics by iron-catalyzed laser-induced graphitization for large-scale applications. Nat Commun, 2022, 13, 3680
[55] Yang Y, Song Y, Bo X, et al. A laser-engraved wearable sensor for sensitive detection of uric acid and tyrosine in sweat. Nat Biotechnol, 2020, 38, 217
[56] Xu G, Jarjes Z A, Wang H W, et al. Detection of neurotransmitters by three-dimensional laser-scribed graphene grass electrodes. ACS Appl Mater Interfaces, 2018, 10, 42136
[57] Getachew B A, Bergsman D S, Grossman J C, et al. Laser-induced graphene from polyimide and polyethersulfone precursors as a sensing electrode in anodic stripping voltammetry. ACS Appl Mater Interfaces, 2020, 12, 48511
[58] You Z, Qiu Q, Chen H, et al. Laser-induced noble metal nanoparticle-graphene composites enabled flexible biosensor for pathogen detection. Biosens Bioelectron, 2020, 150, 111896
[59] Kucherenko I S, Sanborn D, Chen B, et al. Ion-selective sensors based on laser-induced graphene for evaluating human hydration levels using urine samples. Adv Mater Technol, 2020, 5, 1901037
[60] Stanford M G, Zhang C, Fowlkes J D, et al. High-resolution laser-induced graphene. Flexible electronics beyond the visible limit. ACS Appl Mater Interfaces, 2020, 12, 10902
[61] Yoon H, Nah J, Kim H, et al. A chemically modified laser-induced porous graphene based flexible and ultrasensitive electrochemical biosensor for sweat glucose detection. Sens Actuat B, 2020, 311, 127866
[62] Zhao G, Wang F, Zhang Y, et al. High-performance hydrogen peroxide micro-sensors based on laser-induced fabrication of graphene@Ag electrodes. Appl Surf Sci, 2021, 565, 150565
[63] Zhang Y, Li N, Xiang Y, et al. A flexible non-enzymatic glucose sensor based on copper nanoparticles anchored on laser-induced graphene. Carbon, 2020, 156, 506
[64] Prabhakaran A, Nayak P. Surface engineering of laser-scribed graphene sensor enables non-enzymatic glucose detection in human body fluids. ACS Appl Nano Mater, 2020, 3, 391
[65] Torrente-Rodríguez R M, Tu J, Yang Y, et al. Investigation of cortisol dynamics in human sweat using a graphene-based wireless mhealth system. Matter, 2020, 2, 921
[66] Soares R R A, Hjort R G, Pola C C, et al. Laser-induced graphene electrochemical immunosensors for rapid and label-free monitoring of salmonella enterica in chicken broth. ACS Sensors, 2020, 5, 1900
[67] Torrente-Rodríguez R M, Lukas H, Tu J, et al. SARS-CoV-2 rapidplex: A graphene-rased multiplexed telemedicine platform for rapid and low-Cost COVID-19 diagnosis and monitoring. Matter, 2020, 3, 1981
[68] Cardoso A R, Marques A C, Santos L, et al. Molecularly-imprinted chloramphenicol sensor with laser-induced graphene electrodes. Biosens Bioelectron, 2019, 124, 167
[69] Ye R, James D K, Tour J M, et al. Laser-induced graphene: From discovery to translation. Adv Mater, 2019, 3, 1803621
[70] Xu Y, Fei Q, Page M, et al. Laser-induced graphene for bioelectronics and soft actuators. Nano Res, 2021, 14, 3033
[71] Barman S C, Zahed M A, Sharifuzzaman M, et al. A polyallylam-

ine anchored amine-rich laser-ablated graphene platform for facile and highly selective electrochemical IgG biomarker detection. Adv Funct Mater, 2020, 30, 1907297
[72] Cardoso A R, Tavares A P M, Sales M G F, et al. In-situ generated molecularly imprinted material for chloramphenicol electrochemical sensing in waters down to the nanomolar level. Sens Actuat B, 2018, 256, 420
[73] Li Z, Gadipelli S, Li H, et al. Tuning the interlayer spacing of graphene laminate films for efficient pore utilization towards compact capacitive energy storage. Nat Energy, 2020, 5, 160
[74] Simon P, Gogotsi Y. Materials for electrochemical capacitors. Nat Mater, 2008, 7, 845
[75] Khandelwal M, Tran C V, Lee J, et al. Nitrogen and boron co-doped densified laser-induced graphene for supercapacitor applications. Chem Eng J, 2022, 428, 131119
[76] Pomerantseva E, Bonaccorso F, Feng X, et al. Energy storage: The future enabled by nanomaterials. Science, 2019, 366, eaan8285
[77] Li S, Zhang Y, Liu N, et al. Operando revealing dynamic reconstruction of NiCo carbonate hydroxide for high-rate energy storage. Joule, 2020, 4, 673
[78] El-Kady Maher F, Strong V, Dubin S, et al. Laser scribing of high-performance and flexible graphene-based electrochemical capacitors. Science, 2012, 335, 1326
[79] Peng Z, Ye R, Mann J A, et al. Flexible boron-doped laser-induced graphene microsupercapacitors. ACS Nano, 2015, 9, 5868
[80] Clerici F, Fontana M, Bianco S, et al. In situ MoS_2 decoration of laser-induced graphene as flexible supercapacitor electrodes. ACS Appl Mater Interfaces, 2016, 8, 10459
[81] Liu H, Moon K S, Li J, et al. Laser-oxidized Fe_3O_4 nanoparticles anchored on 3D macroporous graphene flexible electrodes for ultrahigh-energy in-plane hybrid micro-supercapacitors. Nano Energy, 2020, 77, 105058
[82] Wu H, Zhang W, Kandambeth S, et al. Conductive metal–organic frameworks selectively grown on laser-scribed graphene for electrochemical microsupercapacitors. Adv Energy Mater, 2019, 9, 1900482
[83] Gao J, Shao C, Shao S, et al. Laser-assisted multiscale fabrication of configuration-editable supercapacitors with high energy density. ACS Nano, 2019, 13, 7463
[84] Yuan Y, Jiang L, Li X, et al. Laser photonic-reduction stamping for graphene-based micro-supercapacitors ultrafast fabrication. Nat Commun, 2020, 11, 6185
[85] Ye J, Tan H, Wu S, et al. Direct laser writing of graphene made from chemical vapor deposition for flexible, integratable micro-supercapacitors with ultrahigh power output. Adv Mater, 2018, 30, 1801384
[86] El-Kady M F, Kaner R B. Scalable fabrication of high-power graphene micro-supercapacitors for flexible and on-chip energy storage. Nat Commun, 2013, 4, 1475
[87] Wang Y, Adekoya D, Sun J, et al. Manipulation of edge-site Fe–N_2 moiety on holey Fe, N codoped graphene to promote the cycle stability and rate capacity of Li–S batteries. Adv Funct Mater, 2019, 29, 1807485
[88] Rambabu A, Senthilkumar B, Sada K, et al. In-situ deposition of sodium titanate thin film as anode for sodium-ion micro-batteries developed by pulsed laser deposition. J Colloid Interface Sci, 2018, 514, 117
[89] Billaud J, Bouville F, Magrini T, et al. Magnetically aligned graphite electrodes for high-rate performance Li-ion batteries. Nat Energy, 2016, 1, 16097
[90] Guo Y, Chen Y, Wang E, et al. Roll-to-Roll continuous manufacturing multifunctional nanocomposites by electric-field-assisted "Z" direction alignment of graphite flakes in poly(dimethylsiloxane). ACS Appl Mater Interfaces, 2017, 9, 919
[91] Shim H C, Tran C V, Hyun S, et al. Three-dimensional laser-induced holey graphene and its dry release transfer onto Cu foil for high-rate energy storage in lithium-ion batteries. Appl Surf Sci, 2021, 564, 150416
[92] Zhang F, Alhajji E, Lei Y, et al. Highly doped 3D graphene Na-Ion battery anode by laser scribing polyimide films in nitrogen ambient. Adv Energy Mater, 2018, 8, 1800353
[93] Chen W, Salvatierra R V, Ren M, et al. Laser-induced silicon oxide for anode-free lithium metal batteries. Adv Mater, 2020, 32, 2002850
[94] Guo J, Zhang W, Yin J, et al. Laser-scribed graphene interlayer for homogeneous zinc deposition and stable zinc-ion batteries. Energy Technol, 2021, 9, 2100490
[95] Jin H, Guo C, Liu X, et al. Emerging two-dimensional nanomaterials for electrocatalysis. Chem Rev, 2018, 118, 6337
[96] Singh S P, Li Y, Zhang J, et al. Sulfur-doped laser-induced porous graphene derived from polysulfone-class polymers and membranes. ACS Nano, 2018, 12, 289
[97] Zhang J, Ren M, Wang L, et al. Oxidized laser-induced graphene for efficient oxygen electrocatalysis. Adv Mater, 2018, 30, 1707319
[98] Ye R, Peng Z, Wang T, et al. In situ formation of metal oxide nanocrystals embedded in laser-induced graphene. ACS Nano, 2015, 9, 9244
[99] Tang Y J, Zheng H, Wang Y, et al. Laser-induced annealing of metal–organic frameworks on conductive substrates for electrochemical water splitting. Adv Funct Mater, 2021, 31, 2102648
[100] Zhang J, Ren M, Li Y, et al. In situ synthesis of efficient water oxidation catalysts in laser-induced graphene. ACS Energy Lett, 2018, 3, 677
[101] Ren M, Zhang J, Tour J M. Laser-induced graphene synthesis of Co_3O_4 in graphene for oxygen electrocatalysis and metal-air batteries. Carbon, 2018, 139, 880
[102] Xu D, Chan K C, Guo H, et al. One-step fabrication of a laser-induced forward transfer graphene/Cu_xO nanocomposite-based electrocatalyst to promote hydrogen evolution reaction. J Mater Chem A, 2021, 9, 16470
[103] Han X, Ye R, Chyan Y, et al. Laser-induced graphene from wood impregnated with metal salts and use in electrocatalysis. ACS Appl Nano Mater, 2018, 1, 5053
[104] Zhang J, Zhang C, Sha J, et al. Efficient water-splitting electrodes based on laser-induced graphene. ACS Appl Mater Interfaces, 2017, 9, 26840
[105] Ren M, Zheng H, Lei J, et al. CO_2 to formic acid using Cu–Sn on laser-induced graphene. ACS Appl Mater Interfaces, 2020, 12, 41223
[106] Nayak P, Jiang Q, Kurra N, et al. Monolithic laser scribed graphene scaffolds with atomic layer deposited platinum for the hydrogen evolution reaction. J Mater Chem A, 2017, 5, 20422
[107] Wu M, Zhang X, Zhao Y, et al. A high-performance hydroxide exchange membrane enabled by Cu^{2+}-crosslinked chitosan. Nat Nanotechnol, 2022, 17, 629
[108] Zhang W, Lei Y, Ming F, et al. Lignin laser lithography: a direct-write method for fabricating 3D graphene electrodes for microsupercapacitors. Adv Energy Mater, 2018, 8, 1801840

Liqiang Zhang is a postdoctoral fellow at Westlake University, School of Engineering. He received his MS and PhD degrees in Zhejiang University of Technology, School of Material Science and Chemical Engineering in 2015 and 2020 respectively. His main research interests including photoelectrocatalytic reduction of CO_2, and electrochemical biosensor.

Ziqian Zhou got her BS and MS degrees from Hunan Agricultural University and South China University of Technology, in 2018 and 2021, respectively. Now she is a PhD student at Westlake University, School of Engineering. Her research focuses on electrocatalysis and biosensor.

Xiaosong Hu is a research associate at the Westlake University, China. He received his PhD degree in Physical Chemistry from Nankai University, China, in 2019. Since 2019, he started his post-doctoral research in School of Engineering, Westlake University. His main research interests include organic/nano catalysis, thermo/electroreduction CO_2 and carbon-based single-atoms materials.

Liaoyong Wen obtained his doctoral degree in applied physics from Technical University of Ilmenau, Germany in 2016. He was then promoted as a senior scientist in the IMN MacroNano® (ZIK), Technical University of Ilmenau. Since 2017, he started his post-doctoral research in Institute of Materials Science, University of Connecticut. Dr. Wen joined the School of Engineering in September 2019 as an assistant professor.